

Rapid antibiotic susceptibility testing and species identification for mixed infections

Vinodh Kandavalli

Uppsala University

Praneeth Karempudi

Uppsala University

Jimmy Larsson

Uppsala University

Johan Elf (✉ johan.elf@icm.uu.se)

Uppsala University <https://orcid.org/0000-0001-5522-1810>

Article

Keywords: antibiotics, antimicrobial resistance, AST, species identification

Posted Date: September 24th, 2021

DOI: <https://doi.org/10.21203/rs.3.rs-892429/v1>

License: © ⓘ This work is licensed under a Creative Commons Attribution 4.0 International License.

[Read Full License](#)

Version of Record: A version of this preprint was published at Nature Communications on October 20th, 2022. See the published version at <https://doi.org/10.1038/s41467-022-33659-1>.

1 Rapid antibiotic susceptibility testing and 2 species identification for mixed infections

3 Vinodh Kandavalli*, Praneeth Karempudi * Jimmy Larsson & Johan Elf#

4 Dept. Cell and Molecular Biology, Uppsala University, Sweden

5

6 *Equal contribution

7 #johan.elf@icm.uu.se

8

9 Abstract

10 **Antimicrobial resistance is an increasing problem globally. Rapid antibiotic susceptibility**
11 **testing (AST) is urgently needed in the clinic to enable personalized prescription in high-**
12 **resistance environments and limit the use of broad-spectrum drugs. Previously we have**
13 **described a 30 min AST method based on imaging of individual bacterial cells. However,**
14 **current phenotypic AST methods do not include species identification (ID), leaving time-**
15 **consuming plating or culturing as the only available option when ID is needed to make**
16 **the sensitivity call. Here we describe a method to perform phenotypic AST at the single-**
17 **cell level in a microfluidic chip that allows subsequent genotyping by *in situ* FISH. By**
18 **stratifying the phenotypic AST response on the species of individual cells, it is possible to**
19 **determine the susceptibility profile for each species in a mixed infection sample in 1.5 h.**
20 **In this proof-of-principle study, we demonstrate the operation with four antibiotics and**
21 **a mixed sample with four species.**

22 Introduction

23 The rapid increase in antibiotic resistance is a serious threat to human health; access to effective
24 antibiotics is a cornerstone of modern medicine and a prerequisite for e.g. cancer treatment and
25 surgery. Different investigations^{1,2} make different estimations of how grave the situation is but
26 there is a consensus view that action needs to be taken or the costs both in terms of human
27 suffering and global economic impact will be staggering³. Experts also agree that the problem
28 is at least partly due to indiscriminate use and misuse of a wide range of antibiotics⁴. To
29 overcome this problem, personalized and rapid antibiotic susceptibility tests (ASTs) are
30 needed, ideally at the point of care⁵. Without these tools, physicians are left with no other option
31 than to prescribe broad-spectrum antibiotics since it can take several days to identify the
32 pathogen(s) and the resistance profile.

33 The limitations of conventional phenotypic ASTs (disk diffusion agar dilution or broth
34 microdilution) are that they require bacterial growth for extended periods in the presence and
35 absence of antibiotics to see an effect. Using standard culture methods, these tests take one day

36 or more to perform but the time can be reduced to 6-10h with automated systems⁶. However,
37 for certain types of bacterial infections, even a delay of 6h before treatment is initiated can have
38 severe consequences⁷. One such example is sepsis, where the risk of death has been estimated
39 to increase by 7.6 % for every hour that effective treatment is not given⁸. Further, it is shown
40 that in the absence of fast AST, more than 25% of septic patients were treated by clinicians
41 with inappropriate antibiotics, which are strongly associated with mortality⁹⁻¹¹. Thus, rapid and
42 accurate ASTs are needed to save lives. However, considering the increases in AMR, life-
43 threatening conditions are not the main culprit, but rather the bulk usage of antibiotics for more
44 benign conditions¹². Resistance is also driven by the strategy to change first-line antibiotics
45 when the local resistance prevalence has reached approx. 10-20%. If fast, reliable ASTs were
46 accessible, high-resistance antibiotics could still be used for the 80-90% of the infections that
47 are still susceptible.

48 The obvious need and benefits of rapid AST, both for saving lives and guiding prescriptions,
49 have resulted in the development of several new methods over the last decade. These methods
50 are described in a number of recent reviews, e.g. ^{4,13}, and we will not repeat all the pros and
51 cons of the different methods here. Briefly, the methods can be divided into genotypic and
52 phenotypic. Genotypic methods identify specific genetic markers that are associated with
53 antibiotic resistance. Although this results in rapid detection of specific resistance genes, it
54 depends on our knowledge of resistance mechanisms which is far from complete¹⁴, in particular
55 considering the rapid emergence of new resistance mechanisms. Furthermore, the absence of
56 resistance genes does not predict susceptibility to antibiotics ¹⁵, i.e., you may learn what not to
57 use but not what will work. In phenotypic methods, the bacteria are exposed to an antibiotic
58 and their phenotypic response, e.g. lysis, growth rate reduction, is monitored. Phenotypic
59 methods work irrespective of the mechanism of resistance. If the phenotypic response is there,
60 the bacterium is susceptible. The various rapid phenotypic AST that have reached the market
61 can deliver an answer (susceptible or resistant) in 2-6h for positive blood cultures that have
62 been growing >6h from sampling the patient. For other samples, e.g. urine, the time-to-answer
63 can be reduced to around 30 min by loading the sample directly into a microchip and measuring
64 the growth-rate with and without antibiotics¹⁶.

65 A common problem for all rapid phenotypic AST methods that assay the patient sample directly
66 without preculture, is that they only work if the species of the bacteria is known ¹⁷. For
67 infections with a narrow spectrum of pathogens, this is not a problem, but for sepsis and other
68 more complex infections, species ID is essential. MALDI-TOF mass spec is currently the
69 golden standard for species determination¹⁸. The technique has until recently only been used
70 for isolated colonies on primary plates, but the practice is changing for blood cultures to remove
71 the additional time of culturing on plates (12h) after the blood culture¹⁹. MALDI-TOF does
72 however require pre-culture of single bacterial species and may not work well for mixed
73 infections commonly seen in sepsis, wounds, catheter-associated UTIs²⁰, and community-
74 acquired pneumonia among others²¹. The challenge remains to make rapid phenotypic AST
75 with species ID that can be used directly on patient samples without a preculture step.

76 To address this issue, we use a microfluidic chip that is capable of rapid capture of individual
77 bacteria from a sample and allows optical monitoring of their growth with and without
78 antibiotics. Next, we identify the bacterial species by fluorescence in situ hybridization (FISH)
79 with species-specific ssDNA probes targeting the 16s/23s rRNA sequence. Once we have the
80 species ID and AST response for each position in the microfluidic chip, we stratify the AST
81 response based on species. A schematic overview of the approach is presented in figure 1.

82 In this proof of principle application, we perform the ASTs for four common pathogens
83 (*Escherichia coli*, *Klebsiella pneumoniae*, *Pseudomonas aeruginosa* as examples of gram-
84 negative strains and *Enterococcus faecalis* as an example of a gram-positive strain) and four
85 different antibiotics from different classes: Vancomycin (Van) [Glycopeptide], Ciprofloxacin
86 (CIP) [Fluoroquinolones], Gentamicin (Gen) [an aminoglycoside], and Nitrofurantoin (NIT)
87 [other agents]. In the end, we show how single-round, multi-color labeling enables
88 identification of up to ten species simultaneously.

89

90 **Results**

91

92 Phenotypic AST followed by Genotyping by FISH.

93 The culture chip that we have developed for this assay is capable of rapid capture of bacteria
94 directly from a liquid sample and allows for optical monitoring of the bacterial growth with
95 and without antibiotics in real time. The same chip design has previously been used to capture
96 bacteria from blood cultures despite an overwhelming excess of blood cells²². The chip features
97 two rows of 3,000 cell traps each. Each trap measures 1.25 x 1.25 x 50 μm ¹⁶ with a constriction
98 at the end which prevents the bacteria from escaping the trap, while still allowing media and
99 probes to flow around the cells. To simulate a mixed infection situation, bacterial overnight
100 cultures of four different species were diluted in a Mueller Hinton (MH) broth, pooled, and
101 directly loaded in the microfluidic chip. In a typical experiment, loading one or a few cells in
102 each trap takes 1 min at $\sim 10^5$ CFU/ml. We supplied growth media with antibiotics to the traps
103 in one of the two rows and plain growth media to the other.

104 The phenotypic response to the antibiotic was determined in ≈ 60 minutes by capturing the
105 phase-contrast images of each cell every 2 min and calculating the growth rates of individual
106 cells. The phenotypic response can be pushed to shorter times depending on which antibiotics
107 are used and at which concentration¹⁶. To identify the species of each bacterial cell, we
108 performed fluorescence *in situ* hybridization (FISH) using species-specific, fluorescent ssDNA
109 probes. These probes bind to the very abundant 16s/23s ribosomal RNA sequences
110 (Supplementary Table 1) and have previously been successfully used for species identification
111 in positive blood cultures²³. The species classification method for FISH signals is described in
112 SI section 3.

113 Analysis using Deep learning models

114 Performing growth rates analysis on multi-species samples requires a general method for
115 detection and tracking of cells that come in different shapes and sizes. It has recently been
116 shown that U-net architecture²⁴ can be used to segment and track *E.coli* cells²⁵ on phase-
117 contrast images with very high accuracy. We performed cell segmentation using the same
118 architecture, trained on *E. coli* and *P. aeruginosa* phase-contrast images paired with ground-
119 truth segmentation masks determined with fluorescent cells (Fig. 2a). In addition to
120 segmentation masks, weight maps (SI fig 1a) were generated to increase the accuracy of cell
121 boundaries between adjacent cells. The training data was heavily augmented to force the
122 network to learn the invariant features that describe a cell on a phase-contrast image. The
123 network performed well on previously unseen species with different shapes and sizes (SI fig.
124 2). An overlay of a predicted segmentation mask on a phase-contrast image with mixed species
125 is shown in figure 2b.

126 Previous approaches to successful *E. coli* tracking have constructed cell-lineages using scoring
127 mechanisms based on overlapping regions¹⁹ or mother-daughter binary mask predictions using
128 full features from the images²⁵. The former approach is very sensitive to tuning overlap
129 parameters while the latter is computationally expensive when a lot of small cells are present
130 in the data. We developed a hybrid approach that performs cell-tracking using a Siamese
131 network²⁶ that scores the similarity between cells from one frame to the next (Fig. 2c). The
132 training of both the segmentation network and the tracking network is described in the
133 supplementary information (sections 1 and 2). Species assignment to tracks was performed
134 after cell-tracking (SI section 5). Figure 2d shows a single segmented mother machine trap
135 tracked through time and the corresponding species-labeled tracks.

136 Species-wise AST response

137 With the species ID and AST response for each position in the microfluidic chip, the species-
138 specific AST response could be determined in the mixed samples. Here, we demonstrate the
139 capability of the method to characterize a mixed sample of four different species, although
140 clinical patient samples are more likely to contain only one or two²⁷⁻²⁹. The AST responses
141 are shown in figure 3a-d. In each experiment, we obtained growth-response curves for three
142 gram-negative strains (*Escherichia coli*, *Klebsiella pneumoniae*, and *Pseudomonas*
143 *aeruginosa*) and one gram-positive strain (*Enterococcus faecalis*). The experiments were
144 performed with four different antibiotics: Vancomycin (Van) [Glycopeptide], Ciprofloxacin
145 (CIP) [Fluoroquinolones], Gentamicin (Gen) [an aminoglycoside], and Nitrofurantoin (NIT)
146 [other agents]. We present the results as response plots from individual experiments to simulate
147 the clinical sample situation and, for comparison, we also display the average responses that
148 would have been the result of the growth-rate measurements without species information.
149 Successful AST-profiling could be achieved with samples containing as little as 100
150 bacteria/species. We used bacteria without specific resistance genes, but since some species
151 have a natural resistance to specific antibiotics, the AST response varies with the species. For
152 example, *Pseudomonas* species are naturally resistant to Ciprofloxacin (Fig. 3a) and
153 Nitrofurantoin (Fig. 3b), and their growth remained unaffected in the presence of 1ug/ml
154 Ciprofloxacin or 32ug/ml Nitrofurantoin. The growth rate of the other bacterial species, on the

155 other hand, dropped more than 10% in 30 min in the presence of these drugs. We also see from
156 the average, non-species-stratified data that without access to species ID, we would not have
157 been able to detect the resistant *Pseudomonas* in the mixed population. Similarly, as expected,
158 all species but *E. faecalis* were found to be susceptible to Gentamicin (2µg/ml) (Fig. 3c) and
159 Vancomycin (4µg/ml) (Fig. 3d).

160 Scaling FISH probing up to 10 species

161 It is estimated that >90% of clinical sepsis samples feature a subset of the 10 most frequent
162 bacterial pathogens³⁰. To increase the number of species that we can identify, we performed
163 combinatorial FISH using a species-specific adaptor that can bind two different fluorescent
164 oligo probes. With probes of four different colors, this set-up can identify up to 10 species (Fig.
165 4a). We demonstrated the combinatorial FISH approach to identify four species loaded in the
166 culture chip (Fig. 4b). Assignment of species was done using k-means clustering on the
167 intensity signal from all four fluorescence channels. Species labels were assigned to clusters
168 manually based on combinations of signals (SI fig 7). Figure 4c shows projections of the
169 clusters in space spanned by the first two principal components of the intensities.
170 Supplementary information section 6 describes this species assignment in detail.

171

172 Discussion

173 In conclusion, we have demonstrated that it is possible to make rapid AST for mixed species
174 infections by performing sequential single-cell phenotypic susceptibility testing and
175 fluorescence *in situ* hybridization in a microfluidic chip. Importantly, ID determination is also
176 applicable for non-mixed infections where it is important to know which MIC-breakpoints to
177 use when making the sensitive-intermediate-resistant call. Although species determination by
178 MALDI-TOF is possible for non-mixed infections and far superior regarding species coverage,
179 this method is limited to centralized hospital labs and samples that are cultured to sufficient
180 biomass. The exact number of cells needed for a MALDI-TOF analysis is hard to find, but it
181 will be orders of magnitude more than what is needed for AST by direct imaging of bacteria.
182 ID with MALDI-TOF will also never be available at the point of care where the majority of
183 antibiotics are prescribed. To guide the initial prescription, it is critical to have the rapid AST
184 as well as sufficiently accurate presumptive species identification near the patient.

185 Since antibiotic susceptibility breakpoints of closely related species are often the same, it can
186 sometimes be enough to distinguish the bacterial family or genera. For example, an
187 Enterobacteriales-specific sequence can cover *Escherichia*, *Klebsiella*, and *Salmonella*, which
188 have very similar resistance breakpoints³¹. This generalization reduces the number of specific
189 probes needed to cover all potential species that can be present in a particular infection.
190 However, if more than 10 specific IDs are required, stripping and reprobing allow for an
191 exponential increase in how many classes can be identified^{32,33}, but at the expense of time.

192 In the current implementation, we ran the test one concentration at a time on a high-end
193 research microscope. To make the technology useful in a clinical setting, the fluidic chip should
194 be parallelized to run multiple antibiotic concentrations simultaneously and with a higher level
195 of automation. Although a minimum of five different concentrations is needed to decide a
196 minimal inhibitory concentration, a simple susceptibility or resistance call can be based on a
197 measurement at a single concentration if the response is well-calibrated to many clinical
198 isolates.

199 **Methods**

200 **Bacterial strains and Antibiotics** In this study, as a gram-negative representative we used *E.*
201 *coli* K12 MG1655, *K. pneumoniae*, and *P. aeruginosa*. As a gram-positive representative, we
202 used *E. faecalis*. We also used the fluorescently tagged *P. aeruginosa* cells, a kind gift from
203 Oana Ciofu³⁴. Antibiotics (Ciprofloxacin, Gentamicin, Nitrofurantoin, and Vancomycin) were
204 purchased from Sigma-Aldrich. Stock solutions were prepared as per the supplier guidelines
205 and stored at -20°C . The solutions were thawed to room temperature before performing the
206 AST experiments.

207 **Media and culture conditions:** In all experiments, Mueller-Hinton (MH) medium (70192;
208 Sigma-Aldrich) was used as a broth. Overnight cultures (ONC) were prepared by inoculating
209 bacteria from glycerol stocks (-80°C) in MH medium and incubating at 37°C for 14-15 hours
210 with continuous shaking (200 rpm). From ONC, cells were diluted 1:1000 times into fresh MH
211 medium supplemented with a surfactant (Pluronic F-108; 542342; Sigma-Aldrich; 0.085%
212 (wt/vol) final concentration). The liquid culture was grown by shaking at 200 rpm at 37°C for
213 2 hours. Next, to perform AST experiments, we mixed the different strains in equal
214 concentrations and loaded them on the microfluidic chip.

215 **The Microfluidic chip and setup:** The chip consist of mainly two parts: a micromolded
216 silicone elastomer [Sylgard 184; polydimethylsiloxane (PDMS)] and a 1.5 mm glass coverslip
217 (Menzel-Gläser) which are covalently bonded together. Chip design and preparation was
218 previously described in^{16,35}. Reference^{16,35} describes the numbering of the ports used below.
219 After punching the ports on the chip, it was placed on the microscope and tubing (TYGON)
220 was connected with a metal tubing connector. Briefly, cells were loaded using the port 8.0 and
221 port 2.0 was used for the exchange of medium with the probes. Ports 5.1, 5.2, and 6.0 were
222 used for maintenance of back channel pressure of 500 mbar, ports 2.1 and 2.2 were used for
223 the supply of MH medium with and without the antibiotics at a pressure of 200 mbar. The
224 pressure was controlled by an OB1-Mk3 pump from Elveflow.

225 **Microfluidic experiments:** Imaging starts within five mins after the supply of medium with
226 and without the antibiotics to the cells. We used a Nikon Ti2-E inverted microscope equipped
227 with a Plan Apo Lambda 100x oil immersion objective (Nikon). Images were captured by the
228 Imaging Source (DMK 38UX304) camera. For phase contrast and fluorescence images, we
229 used the optical setup as previously described in^{16,35} and controlled it by Micro-Manager³⁶, the

230 in-house build plugin. We maintained 30°C as an optimal condition for cells using a
231 temperature controllable unit and a lexan enclosure (Oklab).

232 **Fast phenotypic AST:** Once the cells were loaded on the chip and exposed to growth media
233 with and without the antibiotics, a total of 80-90 positions on each row on the chip were
234 captured in the phase contrast channel (30 ms exposure time) every two mins for an hour.

235 **Genotyping:** After phenotyping, the medium from the ports 2.1 and 2.2 were depressurised to
236 zero. To fix the cells, formaldehyde (4%) was added by opening, switching the medium and
237 applying pressure 200 mbar from port 2.0 for 10 mins and subsequently washing the cells with
238 1 x phosphate buffered saline (PBS) for 5 mins. To permeabilize, cells were treated with 70%
239 EtOH for 10 mins and washed with 1 x PBS (5 mins). Permeabilization of gram-positive cells
240 was done by adding the lysozyme (2 mg/ml) for 3 mins and followed by quick washing with 1
241 x PBS for another 5 mins. For species identification we pooled all specific ssDNA probes
242 (0.1µM) (supplementary table 1) in a hybridization solution (30 % formamide and 2 x SSC)
243 and hybridized for 30 mins at 30°C. Next, we captured the fluorescence images for each
244 individual probe in different channels (TYE 665, TYE 563, Texas Red and Alexa Fluor 488)
245 at 300 ms exposure times and respective phase contrast images at 30 ms exposure time. In total,
246 it took 20 mins to image all the positions in all the channels on the chip.

247 **Cell segmentation and Channel Detection:** Phase-Contrast images of the cells growing in
248 channels were segmented for both cells and channels using a deep learning model with U-net
249 architecture. The cell-segmentation model was trained with data obtained from imaging *E. coli*
250 (K12 MG1655 intC::P70-venusFast) and *P. aeruginosa* strains (PAO1-mCherry-P_{cd}-GFP+)
251 that constitutively express mVenus and GFP respectively. The training procedure was
252 enhanced with data augmentations to force learning features to discriminate cells from the
253 background. The model training and performance on unseen species are described in SI Section
254 1. The channel segmentation model was trained with data that was refined based on histogram
255 profiles, also described in SI Section 2. After obtaining channel locations, time-series stacks of
256 segmented cells and corresponding fluorescent channel images were bundled for tracking,
257 species assignment, and growth rate calculations.

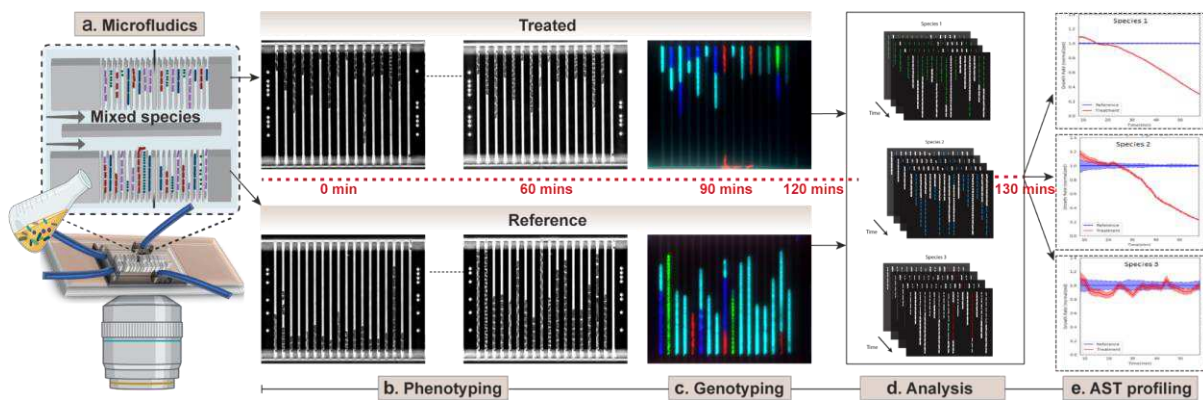
258 **Cell Tracking:** Cells were tracked through time using a neural network that scores similarities
259 between cells from one frame to the next. This neural network has a Siamese net architecture
260 and was trained on a few time-series stacks of multispecies cells that were manually annotated
261 (SI section 4). Cells between frames were linked based on the scores and tracks were generated
262 by chaining a series of links. Cell tracks were corrected for errors (SI section 4).

263 **Species assignment and Growth Curve splitting:** The fluorescent images for each mother
264 machine channel were corrected for background and continuous regions of signal above
265 thresholds were mapped to species labels (SI section 3 and 5). Regions with multiple
266 fluorescent labels for one species were classified using k-means clustering and PCA (SI section
267 6). Cell tracks falling in these regions in the last frame before fixing cells were labeled with the
268 corresponding species and all the species labels were rolled back to time point 0. Growth rates

269 were calculated by fitting exponential curves on the areas of cells in a moving 5 timepoint
270 window (SI section 7).

271 **Oligos and Probes design:** FISH probe sequences for the individual target rRNA were
272 obtained from the Probase^{23,37} and purchased from the Integrated DNA Technologies (
273 www.idt.com), see supplementary table 1. For the combinatorial FISH probing, we used
274 barcode sequence and detection probes, which are listed in supplementary table 2-4, purchased
275 from IDT.

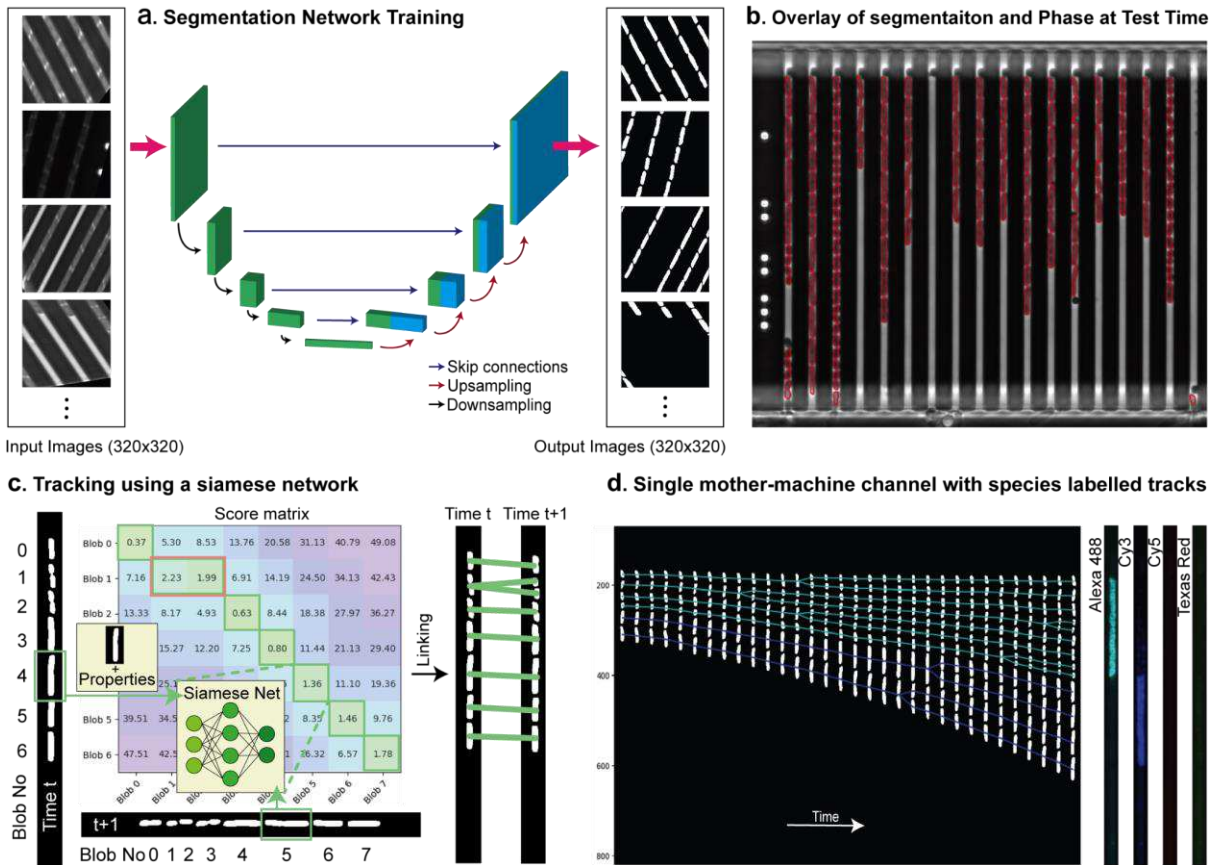
276



277

278 **Figure 1:** Schematic representation of the AST workflow with timeline. a) A cartoon of the
279 microfluidics setup with the mixed species loaded on the chip. b) Time-lapse phase contrast
280 images of the cells in the traps when grown in media with (top) and without (bottom)
281 antibiotics. c) Fluorescence images of the bacteria with ssDNA probes targeting the ribosomal
282 RNA of specific bacteria for species identification. d) Analysis of time-lapse stacks and species
283 ID using deep learning for segmenting and tracking cells. e) Detection of AST profiles for
284 individual pathogens at a given antibiotic concentration.

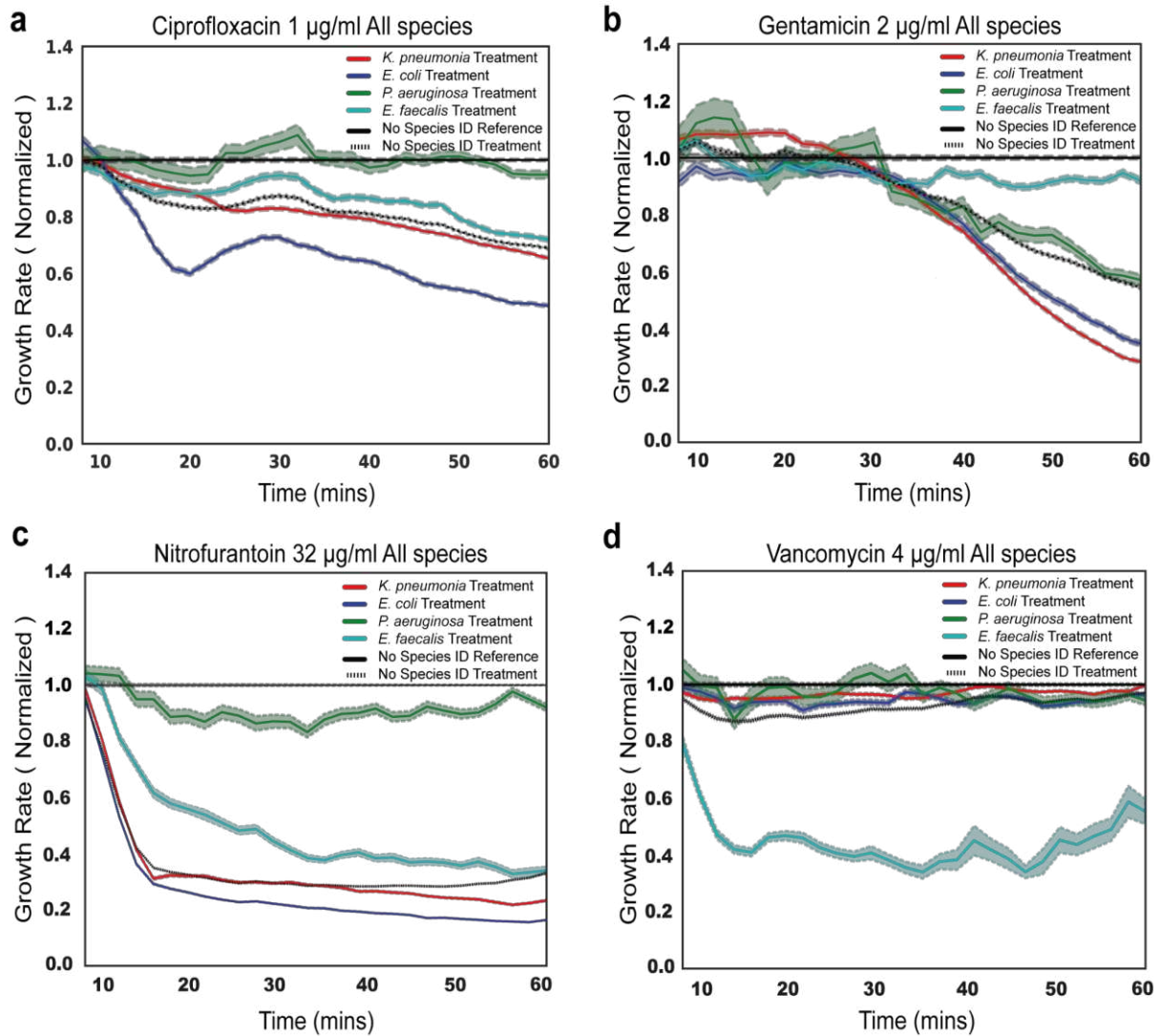
285



286

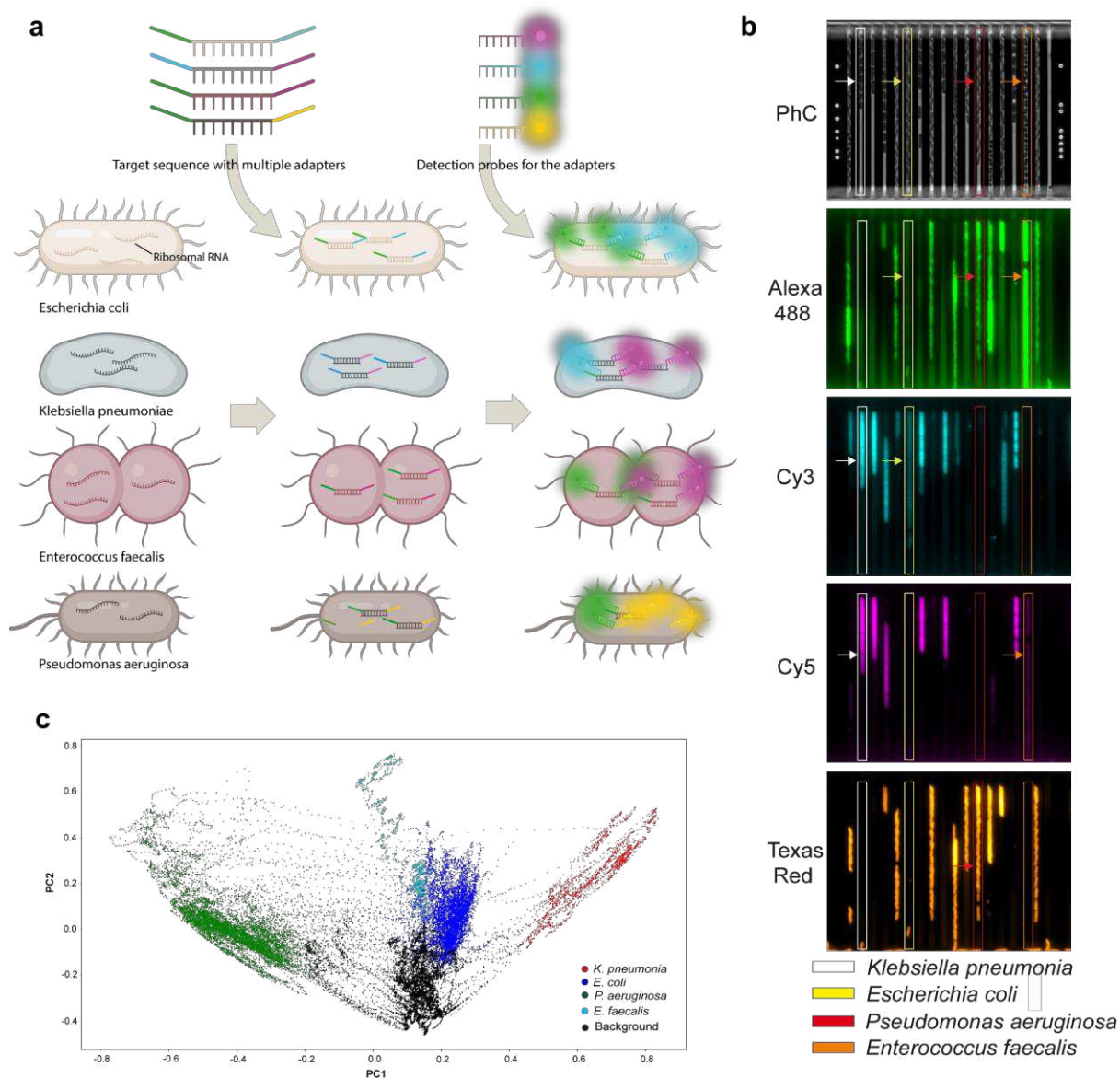
287 **Figure 2:** Analysis a) U-net architecture trained for cell segmentation with corresponding
 288 input-output pairs of images. b) Overlay of contours from the segmentation mask on a phase-
 289 contrast image containing multiple species. c) Each blob from an image at time point t is
 290 compared against all blobs in the next frame at time $t + 1$ to obtain a similarity score (left).
 291 Links between two consecutive frames based on the similarity scores (right). d) A timelapse
 292 stack of segmented cells in a single mother-machine channel and its corresponding
 293 fluorescence images in all four imaging channels. Regions of signal in each fluorescence image
 294 are highlighted with a bounding box (red). Tracks in the last frame falling inside these
 295 bounding boxes are labelled with corresponding species and propagated backward to time $t =$
 296 0. *E. faecalis* tracks with FISH probe in Alexa 488 channel are labeled in cyan and *E. coli*
 297 tracks with FISH probe in Cy3 channel are labeled in blue.

298



299

300 **Figure 3:** Species-wise response to antibiotic treatment. (a-d) AST profiles with normalized
 301 growth rates for the four antibiotics used. The species stratified responses (average and SEM)
 302 as well as the pooled response (without species stratification) is shown for each antibiotic.



303

304 **Figure 4:** *Combinatorial FISH: a) Overview of the combinatorial FISH probing for the multi*
 305 *species identification. A cartoon illustrating the different bacterial species with their ribosomal*
 306 *RNA (left). Illustration of the specific sequences with the multiple adapters targeting the*
 307 *ribosomal RNA of individual bacteria and its hybridization to the target rRNA (middle).*
 308 *Detection probes with different fluorophores. Hybridization of detection probes to the adapter*
 309 *sequences along with unique sequences that are targeted to the species specific rRNA (Right).*
 310 *b) Example images of mixed species loaded in the microfluidic chip and probed using*
 311 *combinatorial FISH for species identification. After the hybridization step, cells were imaged*
 312 *in different channels (PhC, Alexa 488, Cy3, Cy5 and Texas Red). The bacterial species are*
 313 *marked in yellow (Escherichia coli), orange (Enterococcus faecalis), red (Pseudomonas*
 314 *aeruginosa) and white (Klebsiella pneumoniae). c) Clustering of fluorescence imaging*
 315 *intensities using k-means and PCA for species assignment.*

316

317

318 **Acknowledgements** We wish to thank I. Barkefors for helpful input on the manuscript and
319 help with the figures. We acknowledge funding from SSF (ARC19-0016), the European
320 Research Council (BIGGER:885360), the Knut and Alice Wallenberg Foundation (2016.0077;
321 2017.0291; 2019.0439) and the eSSENCE e-science initiative to J.E.

322 **Author contributions.** J.E. conceived the *in-situ* ID after AST method, P.K. developed and
323 implemented the analysis methods and analysed the data. V.K and J.L performed the
324 experiments and developed the protocol for FISH probing in the fluidic chip. J.E., P.K. and
325 V.K. wrote the paper.

326 **Competing interests.** J.E has patented the method (US10,041,104) and founded the company
327 Astrego Diagnostics.

328 **Materials & Correspondence.** All strains, raw data and analysis codes will be provided upon
329 reasonable request to J. E.

330 **References**

- 331 1. GBD 2016 Causes of Death Collaborators. Global, regional, and national age-sex
332 specific mortality for 264 causes of death, 1980-2016: a systematic analysis for the
333 Global Burden of Disease Study 2016. *Lancet* **390**, 1151–1210 (2017).
- 334 2. O’neill. Antimicrobial resistance: tackling a crisis for the health and wealth of nations.
335 Review on antimicrobial resistance. <https://amr-review.org/> (2014).
- 336 3. Review on Antimicrobial Resistance. *Tackling Drug-resistant Infections Globally: Final*
337 *Report and Recommendations*. (2016).
- 338 4. van Belkum, A. *et al.* Innovative and rapid antimicrobial susceptibility testing systems.
339 *Nat. Rev. Microbiol.* **18**, 299–311 (2020).
- 340 5. Schoepp, N. G. *et al.* Rapid pathogen-specific phenotypic antibiotic susceptibility testing
341 using digital LAMP quantification in clinical samples. *Sci. Transl. Med.* **9**, (2017).
- 342 6. Reller, L. B., Weinstein, M., Jorgensen, J. H. & Ferraro, M. J. Antimicrobial
343 Susceptibility Testing: A Review of General Principles and Contemporary Practices.
344 *Clin. Infect. Dis.* **49**, 1749–1755 (2009).
- 345 7. Bernhard, M., Lichtenstern, C., Eckmann, C. & Weigand, M. A. The early antibiotic
346 therapy in septic patients--milestone or sticking point? *Crit. Care* **18**, 671 (2014).
- 347 8. Kumar, A. *et al.* Duration of hypotension before initiation of effective antimicrobial

- 348 therapy is the critical determinant of survival in human septic shock. *Crit. Care Med.* **34**,
349 1589–1596 (2006).
- 350 9. Ibrahim, E. H., Sherman, G., Ward, S., Fraser, V. J. & Kollef, M. H. The influence of
351 inadequate antimicrobial treatment of bloodstream infections on patient outcomes in the
352 ICU setting. *Chest* **118**, 146–155 (2000).
- 353 10. Caliendo, A. M. *et al.* Better tests, better care: improved diagnostics for infectious
354 diseases. *Clin. Infect. Dis.* **57 Suppl 3**, S139–70 (2013).
- 355 11. Kumar, A. *et al.* Initiation of inappropriate antimicrobial therapy results in a fivefold
356 reduction of survival in human septic shock. *Chest* **136**, 1237–1248 (2009).
- 357 12. Ventola, C. L. The antibiotic resistance crisis: part 1: causes and threats. *P T* **40**, 277–
358 283 (2015).
- 359 13. Vasala, A., Hytönen, V. P. & Laitinen, O. H. Modern Tools for Rapid Diagnostics of
360 Antimicrobial Resistance. *Front. Cell. Infect. Microbiol.* **10**, 308 (2020).
- 361 14. Cockerill, F. R. Genetic Methods for Assessing Antimicrobial Resistance. *Antimicrobial*
362 *Agents and Chemotherapy* vol. 43 199–212 (1999).
- 363 15. Bard, J. D. & Lee, F. Why Can't We Just Use PCR? The Role of Genotypic versus
364 Phenotypic Testing for Antimicrobial Resistance Testing. *Clin. Microbiol. Newsl.* **40**,
365 87–95 (2018).
- 366 16. Baltekin, Ö., Boucharin, A., Tano, E., Andersson, D. I. & Elf, J. Antibiotic susceptibility
367 testing in less than 30 min using direct single-cell imaging. *Proceedings of the National*
368 *Academy of Sciences* 201708558 (2017).
- 369 17. Website. The European Committee on Antimicrobial Susceptibility Testing. Breakpoint
370 tables for interpretation of MICs and zone diameters. Version 11.0, 2021.
371 <http://www.eucast.org>.
- 372 18. Rychert, J. Benefits and limitations of MALDI-TOF mass spectrometry for the
373 identification of microorganisms. *J Infectiology* **2**, 1–5 (2019).
- 374 19. Azrad, M. *et al.* Cheap and rapid in-house method for direct identification of positive
375 blood cultures by MALDI-TOF MS technology. *BMC Infect. Dis.* **19**, 72 (2019).
- 376 20. Ferreira, L. *et al.* Direct identification of urinary tract pathogens from urine samples by
377 matrix-assisted laser desorption ionization-time of flight mass spectrometry. *J. Clin.*
378 *Microbiol.* **48**, 2110–2115 (2010).
- 379 21. de Roux, A. *et al.* Mixed community-acquired pneumonia in hospitalised patients. *Eur.*
380 *Respir. J.* **27**, 795–800 (2006).
- 381 22. Özden Baltekin, Uppsala, Sweden Özden Baltekin , Bêrivan Mert , Kajsa Nilsson ,

- 382 Lovisa Söderberg , Martin Lovmar , Volkan Özenci. Evaluation of an ultra-rapid direct
383 antibiotic susceptibility testing (AST) platform on positive blood cultures with
384 *Escherichia coli*. (2019).
- 385 23. Kempf, V. A. J., Trebesius, K. & Autenrieth, I. B. Fluorescent In Situ Hybridization
386 Allows Rapid Identification of Microorganisms in Blood Cultures. *Journal of Clinical*
387 *Microbiology* vol. 38 830–838 (2000).
- 388 24. Ronneberger, O., Fischer, P. & Brox, T. U-Net: Convolutional Networks for Biomedical
389 Image Segmentation. (2015).
- 390 25. Lugagne, J.-B., Lin, H. & Dunlop, M. J. DeLTA: Automated cell segmentation, tracking,
391 and lineage reconstruction using deep learning. *PLoS Comput. Biol.* **16**, e1007673
392 (2020).
- 393 26. Chopra, S., Hadsell, R. & LeCun, Y. Learning a similarity metric discriminatively, with
394 application to face verification. in *2005 IEEE Computer Society Conference on*
395 *Computer Vision and Pattern Recognition (CVPR '05)* (IEEE, 2005).
396 doi:10.1109/cvpr.2005.202.
- 397 27. Wang, J. *et al.* Bacterial species-identifiable magnetic nanosystems for early sepsis
398 diagnosis and extracorporeal photodynamic blood disinfection. *Nanoscale* vol. 10 132–
399 141 (2018).
- 400 28. Charnot-Katsikas, A. *et al.* Use of the Accelerate Pheno System for Identification and
401 Antimicrobial Susceptibility Testing of Pathogens in Positive Blood Cultures and Impact
402 on Time to Results and Workflow. *Journal of Clinical Microbiology* vol. 56 (2017).
- 403 29. Opota, O., Croxatto, A., Prod'homme, G. & Greub, G. Blood culture-based diagnosis of
404 bacteraemia: state of the art. *Clin. Microbiol. Infect.* **21**, 313–322 (2015).
- 405 30. Tabah, A. *et al.* Characteristics and determinants of outcome of hospital-acquired
406 bloodstream infections in intensive care units: the EUROBACT International Cohort
407 Study. *Intensive Care Med.* **38**, 1930–1945 (2012).
- 408 31. EUCAST- European committee on antibiotic susceptibility testing. *Clinical breakpoints*
409 *- breakpoints and guidance* https://www.eucast.org/clinical_breakpoints/.
- 410 32. Lubeck, E., Coskun, A. F., Zhiyentayev, T., Ahmad, M. & Cai, L. Single-cell in situ
411 RNA profiling by sequential hybridization. *Nature methods* vol. 11 360–361 (2014).
- 412 33. Chen, K. H., Boettiger, A. N., Moffitt, J. R., Wang, S. & Zhuang, X. RNA imaging.
413 Spatially resolved, highly multiplexed RNA profiling in single cells. *Science* **348**,
414 aaa6090 (2015).
- 415 34. Zaborskyte, G., Andersen, J. B., Kragh, K. N. & Ciofu, O. Real-Time Monitoring of

- 416 nfxB Mutant Occurrence and Dynamics in *Pseudomonas aeruginosa* Biofilm Exposed to
417 Subinhibitory Concentrations of Ciprofloxacin. *Antimicrobial Agents and Chemotherapy*
418 vol. 61 (2017).
- 419 35. Camsund, D. *et al.* Time-resolved imaging-based CRISPRi screening. *Nat. Methods* **17**,
420 86–92 (2020).
- 421 36. Edelstein, A. D. *et al.* Advanced methods of microscope control using μ Manager
422 software. *Journal of Biological Methods* vol. 1 e10 (2014).
- 423 37. Alm, E. W., Oerther, D. B., Larsen, N., Stahl, D. A. & Raskin, L. The oligonucleotide
424 probe database. *Applied and Environmental Microbiology* vol. 62 3557–3559 (1996).

Supplementary Files

This is a list of supplementary files associated with this preprint. Click to download.

- [ASTsupNatCom.pdf](#)
- [SupplementaryMovies.pptx](#)